Development Of Robust Flight Control Design For Unmanned Aerial Helicopter

May Zin Tun, Zaw Min Naing, Hla Myo Tun

Abstract: A complete flight control scheme with detailed design methodology is proposed for an indoor miniature coaxial helicopter with fixed collective pitch. To avoid system complexity and the problem of minimum phase control, the helicopter dynamic model is decomposed into two cascaded subsystems: an inner one for attitude and heading control and the outer one for trajectory control. H-infinity control technique and robust and perfect tracking method are used to respectively design the inner- and outer-loop controllers. By using the so-called asymptotic time-scale and eigenstructure assignment approach, the design process becomes very systematic and effective. The rotor simulation are also mentioned to improve the stability of UAH. The performance of the autonomous flight control system has been successfully validated in simulation flight tests.

Keywords: UAV, Flight Control, Robust Control, Helicopter, MATLAB

I. INTRODUCTION

Unmanned Aerial Vehicles (UAVs) have attracted significant interests worldwide during the last decade [1]. Among all kinds of UAVs, the miniature coaxial helicopter is one of the most promising platform due to its augmented stability and compact footprint. It is most suitable to fly in confined spaces such as indoor [2]. However, helicopters are more difficult to be controlled than fixed-wing aircraft. They are cross-coupled systems with dynamics changing drastically under different flight conditions. Miniature coaxial helicopters present some unique characteristics different from other types of helicopters, such as more complex aerodynamics of the dual-rotor system and payload limitation on sensors. All these have made the control task complicated and challenging. A few methods have been explored to design autonomous control system for miniature unmanned helicopters [2], [3], [4], [5], [6], [7], [8], [9]. Some of them were only tested by simulation, while some of them consider only parts of the helicopter system. Hence, low-level autonomous control of miniature coaxial helicopters remains a fundamental problem to be solved. Our research team has upgraded several hobby helicopters as autonomous flight testbeds. One of them is from the ESky Big Lama as shown in Fig. 1. Many research works have been done on this platform, including mechanical modification for additional payload, construction of a low cost avionic system for autonomous flight, and nonlinear dynamics modeling for control design and verification [10]. This paper aims to design a complete autonomous control system to stabilize the helicopter and to make it hover in the corner of two walls or fly along a wall. The outline of this paper is as follows. Section II discusses how to formulate the coaxial helicopter system into a dual loop control structure. Section III presents a thorough design procedure of H∞ control for the inner stabilization loop, followed by Section IV, which presents a thorough design procedure of the robust and perfect tracking control for the outer navigation loop. Section V demonstrates the performance of the closed-loop system by carrying out a hovering flight test in the corner of two walls and a forward flight test along a wall. At last, Section VI concludes all the work.

Fig. 1. A Coaxial Helicopter with Fixed Collective Pitch

II. CONTROL SCHEME

With reference to the block diagram shown in Fig. 2, the helicopter has four control inputs: the 'throttle' input u_{thr}, which synchronously increases or decreases the speed of the two rotors and has a direct effect on the heave motion; the 'lateral' input u_{lat}, which dominates the rolling motion and lateral translational motion; the 'longitudinal' input u_{lon}, which dominates the pitching motion and longitudinal translational motion; the 'pedal' input u_{ped}, which differentially alters the speed of the two rotors and thus realizes yawing motion. In our real flight test, a low cost MEMS-based IMU and a short-distance (4 meter) scanning laser range finder (SLRF) are employed to measure the body-axis angular rates, Euler angles, and distance to walls. No velocity information can be obtained directly. In control engineering, the 'divide-and-conquer' strategy is usually used when facing a relatively complex task. In flight control engineering, a natural stratification to the helicopter system is based on motion types, i.e. rotational and translational motion. In general, the dynamics of rotational motion is much faster than that of the translational motion. Thus, the controlled object can be divided into two parts and the overall control system can be formulated in a dual-loop structure. In this way, inner-loop and outer-loop controllers can be designed separately. Moreover, we find that the linearized model of the coaxial helicopter system is of nonminimum phase if the two motion dynamics are combined

together. This will highly complicate the control problem and degrade control performance. Hence, we prefer the dual-loop approach for the design of control laws.

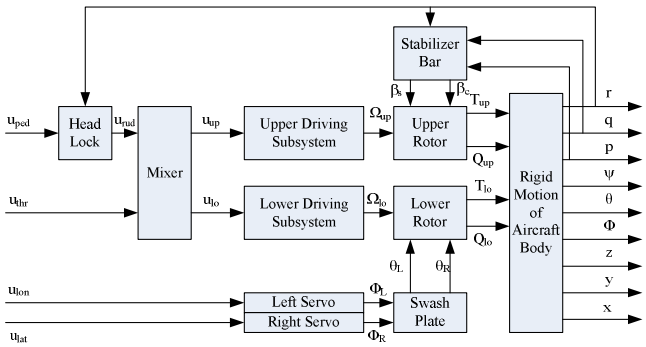

Fig. 2. Block Diagram of A Coaxial Helicopter System

For the inner loop, the controlled object covers the rotational motion of helicopter body, flapping motion of rotor blades and stabilizer bar, rotational motion of the motor-rotor driving system, as well as dynamics embedded within the head-lock gyro. The main task of the inner-loop controller is to stabilize the attitude and heading of the helicopter in all flight conditions. H∞ technique is preferred for robust stability. For the outer loop, the controlled object covers only the translational motion. The main task is to steer the helicopter flying with reference to a series of given locations. A robust and perfect tracking (RPT) approach is implemented for the outer-loop since time factor is important.

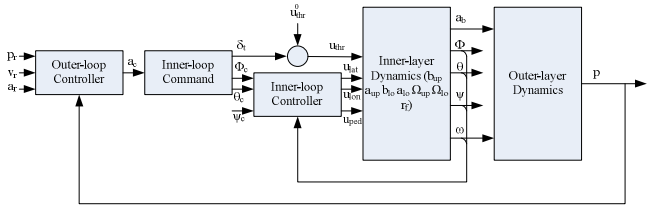

Fig.3. Dual-loop Structure of Flight Control System

It is highlighted that both control laws are designed using the asymptotic time-scale and eigenstructure assignment (ATEA) method, which is fully developed for MIMO LTI systems by Chen et al. [11]. It makes the design process very systematic and effective. To give an overall view, the dual-loop control structure is shown in Fig.3.

III. INNER-LOOP CONTROL DESIGN

The inner-layer dynamics is a 13th-order MIMO system with four control inputs, namely uthr, u_{lat}, u_{lon}, and u_{ped}. To stabilize the attitude and heading angles φ, θ, ψ, only three of the four control inputs u_{lat}, u_{lon}, and u_{ped}, are needed. The remaining one, u_{thr}, is reserved for control of vertical motion and needs to be set at its trimming value (denoted as $u0_{thr}$) while hovering. The system is then a 13th-order 3-input 3-output controlled object. For the measurement part, the IMU gives φ, θ, ψ, p, q, and r. All other state variables (i.e. the four flapping angles b_{up}, a_{up}, b_{lo}, a_{lo}, the two rotational speed Ω_{up}, Ω_{lo}, and the inner state r_f of the head-lock gyro) have to be estimated by an observer. Therefore, the linearized inner layer controlled object can be formulated as

$$\begin{aligned}\dot{x}&=Ax+Bu+Ew\\ y&=C_1x+D_{11}u+D_1w\\ z&=C_2x+D_2u+D_{22}w\end{aligned} \quad (1)$$

with

$x=(\phi\ \theta\ \psi\ p\ q\ r\ b_{up}\ a_{up}\ b_{lo}\ a_{lo}\ \Omega_{up}\ \Omega_{lo}\ r_f)^T$

$y=(\phi\ \theta\ \psi\ p\ q\ r)^T$

$\mathbf{z} = (\varphi\ \theta\ \psi)^T$

$\mathbf{u} = (\delta_{lat}\ \delta_{lon}\ \delta_{ped})^T$

where **y** is the measured output vector, **z** is the controlled output vector, and all variables are the deviations from their trimming values. Note that the direct feedthrough matrices **D**11 and **D**2 are both zeros. No external disturbance is considered for this part of model at the current stage, so the disturbance input matrix **E** and the feedthrough matrices $\mathbf{D}_1$, $\mathbf{D}_{22}$ are both empty. They are reserved in the expression for integrity so that external disturbances such as wind gusts can be considered in future. The controlled subsystem characterized by quadruple (**A**, **B**, $\mathbf{C}_2$, $\mathbf{D}_2$) is both observable and controllable. By transforming the quadruple into the special coordinate basis (SCB) form [11], we find that the subsystem is invertible and of minimum phase with 4 stable invariant zeros and 3 infinite zeros of order 3. Hence, we can design an H∞ controller via the ATEA method using state feedback to obtain robust stability. After that, an observer-based controller can be designed utilizing measurement feedback also via the same method. Usually, the control law designed via the ATEA method is parameterized by a number $\gamma > \gamma^*$, where γ^* is the infimum of the H∞-norm of the closed-loop transfer matrix from disturbance **w** to controlled output **z**. We will find that our design result does not depend on the number γ because the controlled subsystem (**A**, **B**, $\mathbf{C}_2$, $\mathbf{D}_2$) is right invertible and of minimum phase, and the measurable subsystem (**A**, **E**, $\mathbf{C}_1$, $\mathbf{D}_1$) is left invertible and of minimum phase. This simplifies the design process significantly.

A. H∞ State Feedback Control Design

It can be realized step-by-step via the ATEA method as follows. First, transform the matrix quadruple (**A**, **B**, $\mathbf{C}_2$, $\mathbf{D}_2$) of the controlled subsystem into its SCB form

$$\tilde{A}=\begin{bmatrix} A_{aa}^{-} & L_{ad}^{-}C_d \\ B_dE_{da}^{-} & A_{dd}\end{bmatrix}\quad \tilde{B}=\begin{bmatrix}0\\ B_d\end{bmatrix}\quad \tilde{C}=[0\quad C_d] \quad (2)$$

With

$A_{dd}=A_{dd}^{*}+B_dE_{dd}+L_{dd}C_d$

by state, output, input transformations $\mathbf{T}_{s1}$, $\mathbf{T}_{o1}$, $\mathbf{T}_{i1}$. Because the subsystem is invertible and of minimum phase, only the infinite eigenstructure need be assigned explicitly. Second, the subsystem related to the infinite zero structure has 3 infinite zeros of order 3, i.e. there are 3 chains of integrators from the 3 control inputs to the 3 controlled outputs and each chain is composed of 3 integrators in series. The desired characteristic functions of the 3 subspaces can be set as

$$p_1(s) = s^3 + a_{11}s^2 + a_{12}s + a_{13} \quad (3)$$
$$p_2(s) = s^3 + a_{21}s^2 + a_{22}s + a_{23} \quad (4)$$
$$p_3(s) = s^3 + a_{31}s^2 + a_{32}s + a_{33} \quad (5)$$

with their eigenvalues assigned respectively at (–3.4401,–2.4787 ± 7.4778i), (–3.8962, –0.9846 ± 4.0397i), and (–1.5, –4 ± 11i), which correspond to roll, pitch, and yaw

control channels respectively. Thus, the time-scale assignment is as follows

$$F_d=\begin{bmatrix} \frac{a_{13}}{\epsilon^3} & \frac{a_{12}}{\epsilon^2} & \frac{a_{11}}{\epsilon^1} & 0 & 0 & 0 & 0 & 0 & 0 \\ 0 & 0 & 0 & \frac{a_{23}}{\epsilon^3} & \frac{a_{22}}{\epsilon^2} & \frac{a_{21}}{\epsilon^1} & 0 & 0 & 0 \\ 0 & 0 & 0 & 0 & 0 & 0 & \frac{a_{33}}{\epsilon^3} & \frac{a_{32}}{\epsilon^2} & \frac{a_{31}}{\epsilon^1} \end{bmatrix} \quad (6)$$

Finally, the composite state feedback gain by structural assignment is given as

$$\mathbf{F}_s = -T_{i1}([0\ \mathbf{F}_d] + [\mathbf{E}^{-}_{da}\ \mathbf{E}_{dd}])\mathbf{T}^{-1}_{s1} \quad (7)$$

IV. Outer-Loop Control Design

Hovering in the corner of two walls or flying along a wall are two basic tasks for indoor flight. This section tries to design the hovering and wall-following control for the indoor miniature coaxial helicopter. We have partitioned the whole dynamic model of our aircraft into two parts and have finished the inner-loop design which stabilizes attitude and heading. The outer-loop control can then be designed separately and based on the dynamic model of aircraft's translational motion only, provided that the outer loop is slow enough as compared to the inner loop. Furthermore, the translational model can be divided into two parts: trajectory kinematics and trajectory dynamics. The kinematics part can be described in different coordinate systems, such as a North-East-Down (NED) coordinate system or a body-carried coordinate system. In our implementation, the positioning sensor is a SLRF, so global NED coordinates of aircraft are unknown and only the local distance information is obtained relative to the walls (see Fig. 4). In the figure, the thick line represents the wall to be followed; $o_nx_ny_nz_n$ stands for an NED coordinate system which is usually fixed at the starting point of flight and approximates the inertial frame of reference; $o_bx_by_bz_b$ stands for the body-axis coordinate system as the conventional definition in aeronautical engineering; $o_wx_wy_wz_w$ stands for the so called local-wall coordinate system which is defined as follows. Its origin o_w is set at the intersection of the wall with the perpendicular line passing through ob, x_w-axis is along the wall spanning an acute angle with x_b-axis, y_w-axis is along the perpendicular line pointing to ob. In flight, we don't know the position and velocity of ob in the NED coordinate system, but only the information with respect to the local-wall coordinate system. In this case, we have to describe and design the outer navigation loop in the body-axis coordinate system. Let $\mathbf{p} = (x, y, z)^T$, $\mathbf{v} = (u, v, w)^T$, $\mathbf{a} = (a_x, a_y, a_z)^T$ be the position, velocity, acceleration of the helicopter with respect to the local-wall coordinate system. With reference to the kinematics of moving reference of frames, the trajectory kinematics of our helicopter is described in the body-axis coordinate system as follows,

$$\mathbf{p}^{\cdot b} = \mathbf{p}^{\cdot n} - \boldsymbol{\omega} \times \mathbf{p} = \mathbf{v} - \boldsymbol{\omega} \times \mathbf{p} \quad (8)$$

$$\mathbf{v}^{\cdot b} = \mathbf{v}^{\cdot n} - \boldsymbol{\omega} \times \mathbf{v} = \mathbf{a} - \boldsymbol{\omega} \times \mathbf{v} \quad (9)$$

where the superscripts ^{b} and ^{n} means that the differentiation is performed in the body-axis and NED coordinate systems respectively, $\boldsymbol{\omega} = (p, q, r)^T$ is the angular velocity of aircraft body. The above equations are then linearized as

$$\dot{\delta_p}^b=\delta v-[\omega^0]_\times \delta p+[p^0]_\times \delta\omega \quad (10)$$

$$\dot{\delta_v}^b=\delta a-[\omega^0]_\times \delta v+[v^0]_\times \delta\omega \quad (11)$$

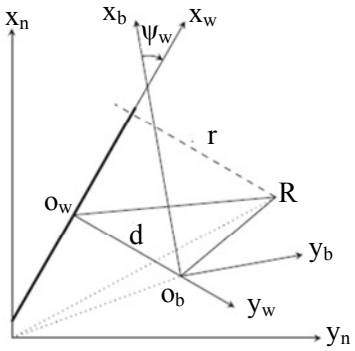

Fig. 4. Outer-loop Reference Generation for Flight along a Wall

where $\mathbf{p}^0$, $\mathbf{v}^0$, $\boldsymbol{\omega}^0$ are respectively the position, velocity, angular velocity at the operating points for linearization, $[\cdot]_\times$ is the anti-skew matrix spanned by the vector inside the brackets. Hereafter, for the economy of notations, the prefix δ representing variable deviation and the superscript ^{b} will be omitted if without ambiguity. Notice that $\mathbf{a} = \mathbf{a}_b - \mathbf{a}_w$, where $\mathbf{a}_b$ and $\mathbf{a}_w$ are the acceleration of aircraft body and the wall coordinate system with respect to the NED coordinate system. The acceleration $\mathbf{a}_b$ is one of the outputs from the inner-layer helicopter model whereas $\mathbf{a}_w$ is unknown. Besides, we should know that instead of angular velocity $\boldsymbol{\omega}$, acceleration $\mathbf{a}_b$ is the dominant input to the trajectory kinematics. Thus, let $\mathbf{p}$ and $\mathbf{v}$ be the states of the trajectory kinematics, $\mathbf{a}_b$ be the control input, we have the following form

$$\begin{pmatrix}\dot{p}\\ \dot{v}\end{pmatrix}=\begin{bmatrix}-[\omega^0]_\times & I\\ 0 & -[\omega^0]_\times\end{bmatrix}\begin{pmatrix}p\\ v\end{pmatrix}+\begin{bmatrix}0\\ I\end{bmatrix}a_b+\begin{bmatrix}[p^0]_\times & o\\ [v^0]_\times & -I\end{bmatrix}\begin{pmatrix}\omega\\ a_w\end{pmatrix} \quad (12)$$

where $\boldsymbol{\omega}$ and $\mathbf{a}_w$ as the external disturbance. It can be represented compactly as

$$\mathbf{x}^{\cdot}_o = \mathbf{A}_o\mathbf{x}_o + \mathbf{B}_o\mathbf{u}_o + \mathbf{E}_o\mathbf{w}_o \quad (13)$$

and so called outer-layer dynamics in this paper. For the measurement, only position of the helicopter with respect to the walls can be acquired. By finite difference, we can also get the velocity of our helicopter. Although finite difference usually enlarges noises, it does work properly by simple filtering. Hence, we use this technique to obtain velocity estimation at the current stage. In future, a proper observer may be designed. Therefore, we get the measured and controlled output equations of the outer-layer model,

$$y=C_1x_0=\begin{bmatrix}I & 0\\ 0 & I\end{bmatrix}\begin{pmatrix}p\\ v\end{pmatrix} \quad (14)$$

$$z=C_2x_0=[I\quad 0]\begin{pmatrix}p\\ v\end{pmatrix} \quad (15)$$

Equation (13), (14), (15) constitute the controlled object of the outer-loop design. Specifically,

$$A_0=\begin{bmatrix}0 & I\\ I & 0\end{bmatrix} \quad (16)$$

since $\boldsymbol{\omega}^0$ is zero in hovering and forward flight conditions. Due to the decoupled characteristics of the outer-layer model, i.e. there are three control channels independent of each other, we can design the overall outer-loop control law based on the three decoupled SISO models

V. IMPLEMENTATION

Several flight tests have been conducted to validate the proposed control scheme. We present here two simple but representative scenarios: hovering in the corner of two walls and forward flight along a wall.

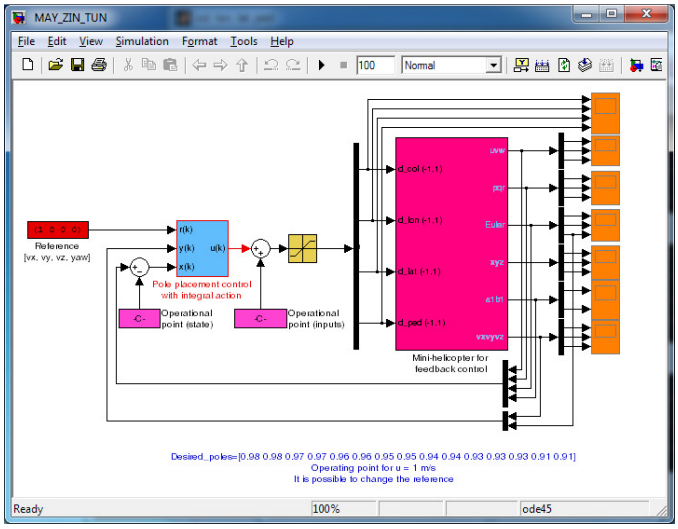

Fig.5. SIMULINK Model for Coaxial Helicopter

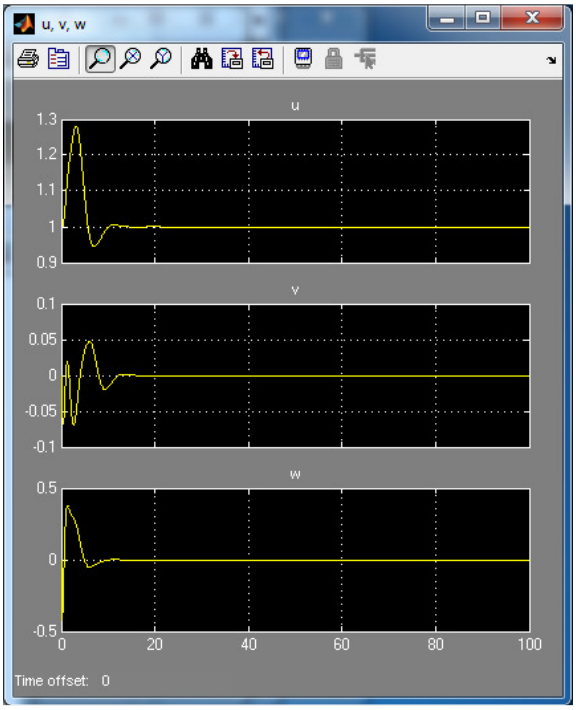

Fig.6. Translational velocity components of helicopter along fuselage axis (m/s)

The reference generation for the whole control system must be consistent with our RPT controller. That is, the position reference $\mathbf{p}_r$, velocity reference $\mathbf{v}r$ and acceleration reference $\mathbf{a}_r$ should all be calculated and properly assigned. Fig.6 shows the translational velocity components of helicopter along fuselage axis (m/s). The response of u,v and w says the acceptable range of less than 20 ms for hovering stage.

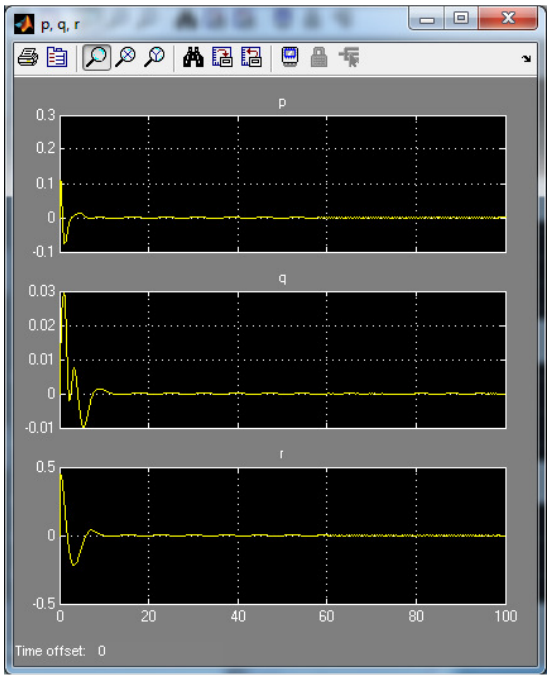

Fig.7. Angular velocities components of helicopter

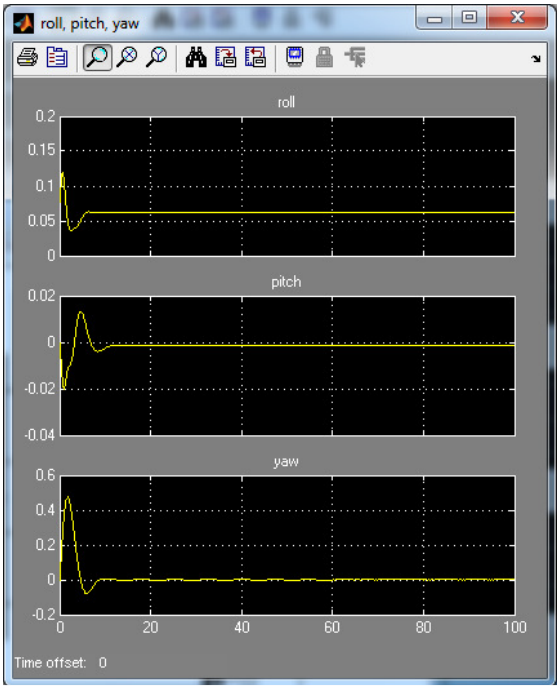

Fig.8. Euler angles defining the orientation of the aircraft relative to the Earth (rad)

Fig.7 describes the angular velocities components of helicopter. The values of p,q and r state the tolerable assortment of stability point under 10 ms for simulation test.

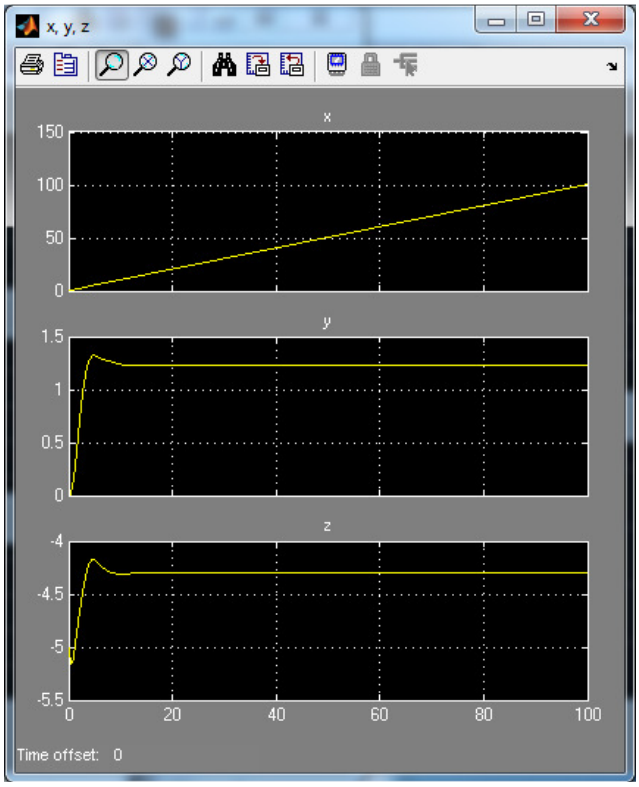

Fig.9. External aerodynamic forces in x,y,z body axes (N, lb)

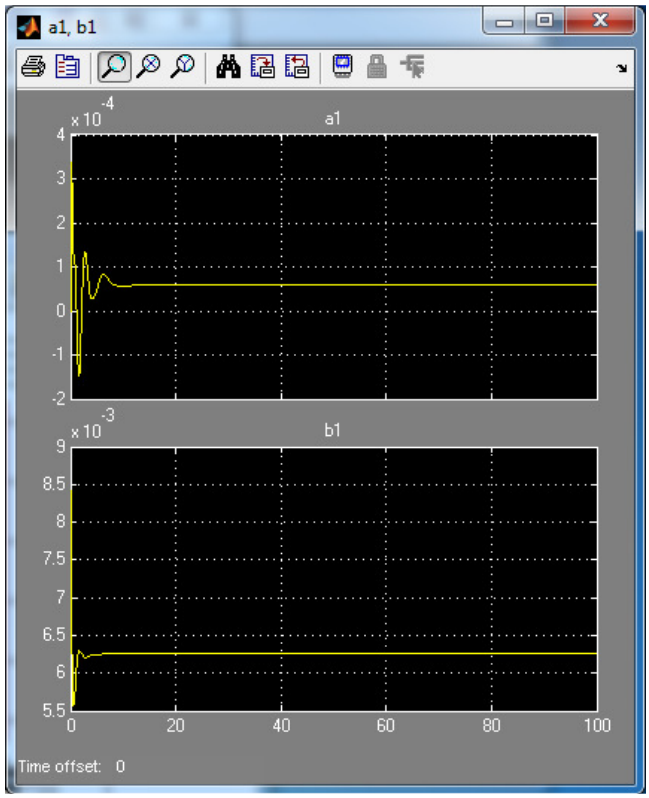

Fig.10. State Responses for A and B

Fig.8 mentions the Euler angles defining the orientation of the aircraft relative to the Earth (rad). The roll rate, yaw rate and pitch rate are also point out the endurable variety of permanence position less than 10 ms for analysis. Fig.9 illustrates the external aerodynamic forces in x,y,z body axes (N, lb). For hovering condition, the value of x can be ramp situation; the values of y and z have to be approached to specified level for stability condition. Fig.10 shows the state responses for A and B and Fig.11 illustrates the translational velocity components of helicopter along with x,y and z axis (m/s).

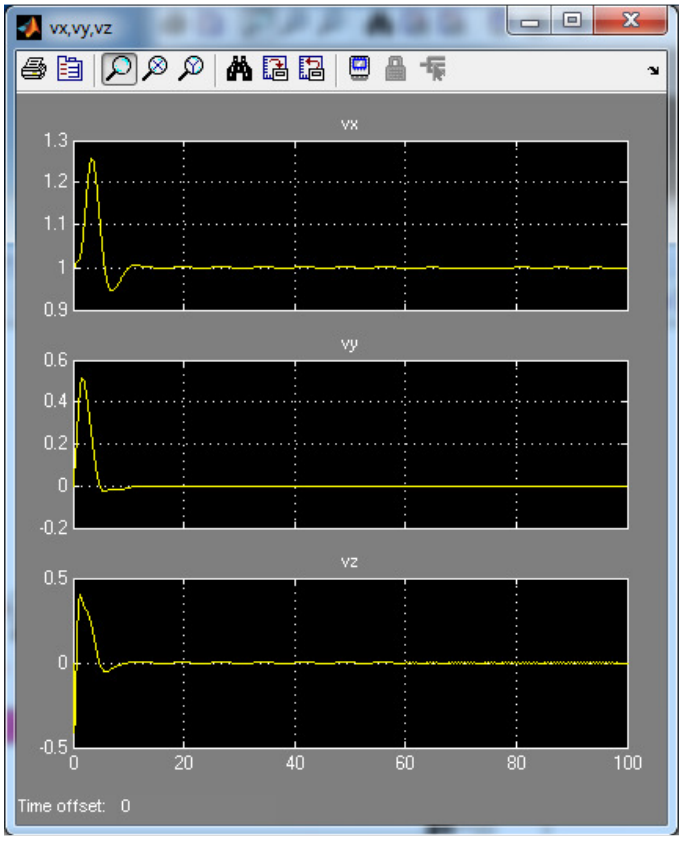

Fig.11. Translational velocity components of helicopter along with x,y and z axis (m/s)

VI. ROTOR SIMULATION

In this part, we can simulate the rotor movement and stability condition for main rotor based on the zero and first harmonics (in Degree). The analyzed parameters for beta, theta and zeta are assigned by the following.

Beta=[0 15 0]
Theta=[5 12 10]
Zeta=[0 0 0]

According to the simulation parameters from zero and first harmonics (in Degree), the rotor simulations for various condition are demonstrated. Fig 12 shows the iso-view of rotor simulation for 250 degree. Fig.13 mentions the same view of rotor simulation for 45 degree and Fig 14 illustrates the xy view of Fig.13. The rotor movement is depending on the analyzed parameter for simulation approach for UAH.

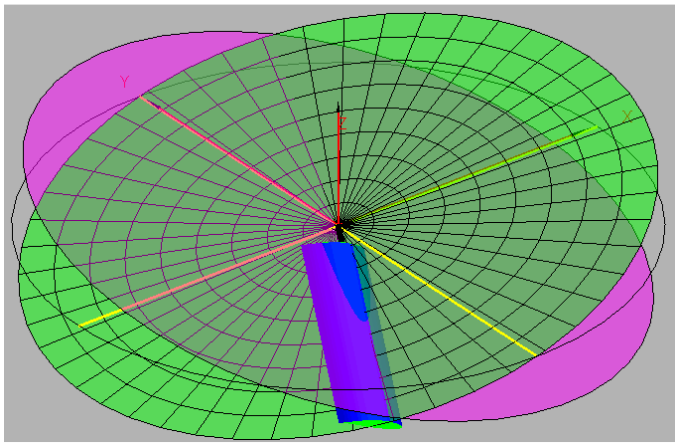

Fig 12. The Iso-view of Rotor Simulation for 250 Degree

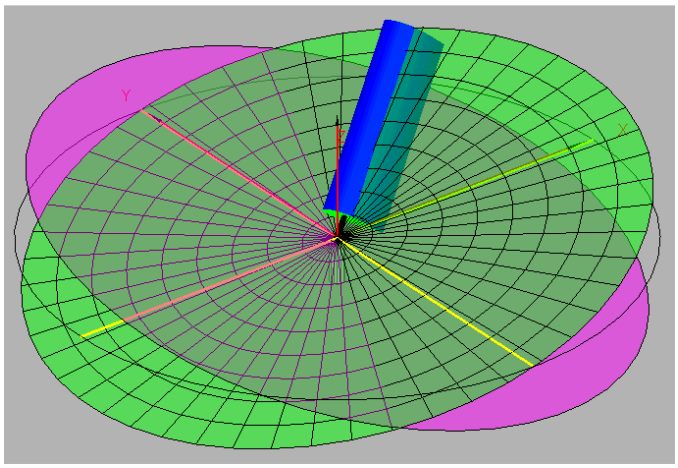

Fig 13. The Iso-view of Rotor Simulation for 45 Degree

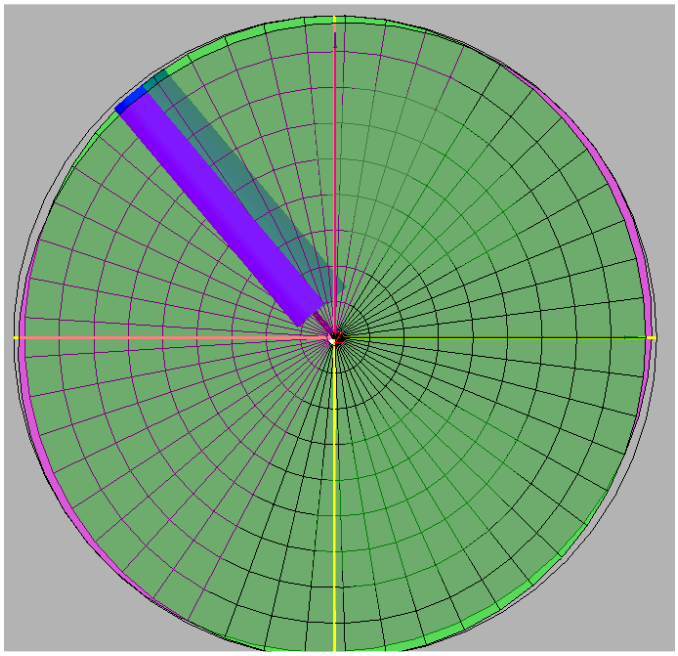

Fig 14. The xy-view of Rotor Simulation for 45 Degree

VII. CONCLUSIONS

The paper has presented a complete and systematic method to design a flight control system for a coaxial helicopter. The overall design is based on a dual-loop structure so that complexity is reduced and the non-minimum phase problem is avoided. Control laws for both inner and outer loops are designed using the asymptotic time-scale and eigenstructure assignment method, which keeps the procedure effective and unified. Indeed, the whole approach is also extendible to autonomous control of other types of helicopters, even for fixed-wing aircraft. From the flight test results, it is found that air drag to the rotor system is not negligible. In the next stage, this air drag effect will be investigated and added to the dynamic model. Based on the new model, control laws, thus controlled performance is expected to be improved. On the other hand, measurement is another area that deserves refinement. The rotor simulations are also developed for stability analysis of UAH.

ACKNOWLEDGMENT

I would wish to acknowledge the many colleagues at Mandalay Technological University who have contributed to the development of this paper.

REFERENCES

[1] K. Nonami, F. Kendoul, S. Suzuki, W. Wang, and D. Nakazawa, Autonomous Flying Robots: Unmanned Aerial Vehicles and Micro Aerial Vehicles, Springer, 2010.

[2] H. Lim and S. Machida,“Mechanism and Control of Coaxial Double Contra-Rotation Flying Robot,” in Proceedings of International Conference on Control, Automation and System, Gyeonggi-do, Korea, October 27-30, 2010, pp. 1109-1114.

[3] P. Fankhauser, S. Bouabdallah, S. Leutenegger, and R. Siegwart, “Modeling and Decoupling Control of the CoaX Micro Helicopter,” in Proceedings of IEEE/RSJ International Conference on Intelligent Robots and Systems, San Francisco, USA, September 25-30, 2011, pp.2223-2228.

[4] D. Schafroth, C. Bermes, S. Bouabdallah, and R.Siegwart, “Modeling, System Identification and Robust Control of a Coaxial Micro Helicopter,” Control Engineering Practice, Vol. 18, pp. 700-711, 2010.

[5] B. Vidolov, J. De Miras, and S. Bonnet, “A Two-Rule-Based Fuzzy Logic Controller for Contrarotating Coaxial Rotors UAV,” in Proceedings of IEEE International Conference on Fuzzy Systems, Vancouver, Canada, July 16-21, 2006, pp. 1563-1569.

[6] S. P. Soundararaj, A. K. Sujeeth, and A. Saxena, “Autonomous Indoor Helicopter Flight using a Single Onboard Camera,” in Proceedings of IEEE/RSJ International Conference on intellegent Robtos and Systems, St. Louis, USA, October 11-15, 2009, pp. 5307-5134.

[7] S. Wu, Z. Zheng, and K. Cai, “Indoor Autonomous Hovering Control for a Small Unmanned Coaxial

Helicopter," in Proceedings of the 8th IEEE International Conference on Control and Automation, Xiamen, China, June 9-11, 2010, pp. 267-272.

[8] H. Wang, D. Wang, X. Niu, and H. Duan, "Modeling and Hovering Control of a Novel Unmanned Coaxial Rotor/Ducted-Fan Helicopter," in Porceedings of IEEE International Conference on Automation and Logistics, Jinan, China, August 18-21, 2007, pp.1768-1773.

[9] B. Arama, S. Barissi, and N. Houshangi, "Control of an Unmanned Coaxial helicopter Using Hybrid Fuzzy-PID Controllers," in Proceedings of the 24th Canadian Conference on Electrical and Computer Engineering, Niagara Falls, Canada, May 8-11, 2011, pp. 1064-1068.

[10] F. Wang, S. K. Phang, J. Cui, B. M. Chen, T. H. and Lee, "Nonlinear Modeling of a Miniature Fixed-Pitch Coaxial UAV," accepted by the 2012 American Control Conference.

[11] B. M. Chen, Robust and H∞ Control, London: Springer-Verlag, 2000.